Macromolecular Research

Article

DOI 10.1007/s13233-017-5104-y

www.springer.com/13233 pISSN 1598-5032 eISSN 2092-7673

Synthesis of Conjugated Polymer Nanoparticles with Core-Shell Structure for Cell Imaging and Photodynamic Cancer Therapy

Choongho Kim[1]
Sun-Young Kim[2]
Yong Taik Lim[2]
Taek Seung Lee*[,1]

[1] Organic and Optoelectronic Materials Laboratory, Department of Organic Materials Engineering, Chungnam National University, Daejeon 34134, Korea
[2] SKKU Advanced Institute of Nanotechnology (SAINT), Sungkyunkwan University, 2066 Seobu-ro, Jangan-gu, Suwon, Gyeonggi 16419, Korea

Received March 27, 2017 / Revised May 5, 2017 / Accepted May 7, 2017

Abstract: Conjugated polymer nanoparticles were successfully capped with a commercially available triblock copolymer Pluronic F127® to form stable nanoparticles with the potential for photodynamic therapy (PDT) of cancer cells. PDT is known as an effective, simple treatment method without the need for surgery. Investigations on the particle structure revealed that the nanoparticles were fabricated with a core-shell structure of ~192 nm. The PDT effects of the nanoparticles on HeLa cancer cells were investigated *via* cell imaging and cytotoxicity tests. The nanoparticles were biocompatible and were easily internalized by HeLa cells. Moreover, the nanoparticles efficiently generated reactive oxygen species to kill cancer cells under UV irradiation. Therefore, the nanoparticles have promising applications for cancer cell imaging and therapy.

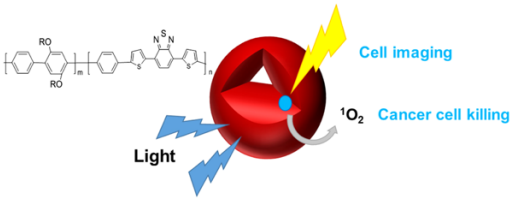

Keywords: conjugated polymer nanoparticles, cancer cells, imaging, photodynamic therapy, reactive oxygen species.

1. Introduction

Health is a major concern in modern society and thus its related fields are continuously developing. Cancer, one of the most serious threats to human health, is a difficult disease to treat and numerous studies have been conducted worldwide to investigate the treatment of cancer diseases.[1-3] Recently, as potential approaches for minimally invasive treatment of various malignant cancers, photothermal therapy and photodynamic therapy (PDT) have received much attention because they can avoid detrimental effects on normal cells.[4-6] PDT, in particular, has attracted considerable interest as an efficient treatment for cancer cells and other diseases.[7,8] The PDT method benefits from the process in which light is absorbed by a photosensitizer (PS) and the light-sensitive PS converts the optical energy to generate reactive oxygen species (ROS) including singlet oxygen ($^1O_2$) to induce cancer cell death. ROS attack cells with their strong oxidizing ability. PDT is seen as attractive because of its minimal invasiveness, high specificity, and low toxicity for normal cells. In particular, ROS-based PDT is facilitated by the absorption of various light energies.[9-12]

Recent investigations on conjugated polymers (CPs) have enabled them to be used in biological fields such as biosensing, drug delivery, and cell imaging when they are soluble (or finely-dispersible) in water.[13-18] CPs can produce ROS under light irradiation to kill cancer cells.[19-22] As a PS, CP nanoparticles have been used for the creation of a photodymanic effect in cells and in aqueous solutions.[23-25] The advantages of CP nanoparticles lie in their excellent biocompatibility, ease of surface modification, high quantum yield, high brightness, and good photostability.[26-28] As a result, PDT using CP nanoparticles is seen as an effective medical treatment for a variety of diseases including cancer. However, most of the investigations on CP nanoparticles for the PD effect were related to the use of additional PSs, including phthalocyanine and lanthanides, which need complicated synthetic work.[29,30] Moreover, CP nanoparticles themselves have difficulty in uptake by cancer cells because they usually have negative charges on the surface and intrinsic hydrophobicity, requiring surface-treatment of the CP to diffuse into cancer cells.

To encapsulate such hydrophobic materials for better cellular uptake and drug delivery, Pluronic block copolymers have been widely used to form self-assembled polymeric micelles that can dramatically enhance water-solubility, bioavailability, and stability.[31,32] Pluronic block copolymers are composed of hydrophilic ethylene oxide (EO) and hydrophobic propylene oxide (PO), resulting in an amphiphilic structure.[33-35]

Here, we constructed CP nanoparticles covered with Pluronic block copolymers to obtain red-emitting PBTB-F. The decoration with Pluronic copolymer enabled PBTB-F to internalize easily in cancer cells. The PBTB-F facilitated the imaging of cancer cells by diffusing into the cytoplasm and could also be applied in facile cancer-cell PDT, demonstrating versatile uses in cancer diagnosis and treatment. Cancer cell death was effectively induced by cell apoptosis through PDT under ultraviolet (UV) light irradiation. Compared with previous studies of PDT with CP nanoparticles, our system does not require additional pho-

Acknowledgments: Financial support from the National Research Foundation of Korea (NRF) funded by Korean government through the Nuclear R&D Project (2015M2A7A1000217) is gratefully acknowledged.

***Corresponding Author:** Taek Seung Lee (tslee@cnu.ac.kr)

© The Polymer Society of Korea and Springer 2017

tosensitizing compounds. Thus, the simple use of the PBTB-F facilitated apoptosis of cancer cells by releasing active oxygen in response to light irradiation.

2. Experimental

2.1. Reagents and Characterization

Monomers for Suzuki cross-coupling polymerization, such as 1,4-dibromo-2,5-bis(octyloxy)benzene (**2**) and 4,7-bis(5-bromo-2-thienyl)-2,1,3-benzothiadiazole (**5**) were synthesized according to previously published methods.[36,37] 2,1,3-Benzothiadiazole, hydroquinone, potassium hydroxide, potassium carbonate, tetrakis (triphenylphosphine) palladium, p-nitroso-N,N'-dimethylaniline (RNO), and Pluronic F127 were purchased from Sigma Aldrich and used as received. 2',7'-Dichlorodihydrofluorescein diacetate (H2DCFDA) was purchased from Molecular Probes/Invitrogen. ^{1}H and ^{13}C NMR were recorded on a Bruker DRX-300 spectrometer with tetramethylsilane as an internal standard (Korea Basic Science Institute). FT-IR spectra were obtained using a Bruker Tensor 27 spectrometer. UV-vis spectra were recorded on a PerkinElmer Lambda 35 spectrometer. Photoluminescence spectra were obtained using a Cary Eclipse fluorescence spectrophotometer equipped with a xenon lamp. Elemental analysis (EA) was performed on an EA 1108 elemental analyzer (Fisons Instruments). The images of nanoparticles were obtained using a field-emission scanning electron microscope (FE-SEM; Hitachi S-4800) and the size of the nanoparticles was determined by dynamic light scattering (DLS; Malvern Zetasizer). Gel permeation chromatography (GPC) was used to determine the molecular weight of the polymer with polystyrene standards using tetrahydrofuran (THF) as the eluent. Fluorescence images of cancer cells were obtained using a DeltaVisionTM PD system. The nanoparticles were UV irradiated with a Spectrolinker XL-1000 UV lamp (Spectronics Corporation).

2.2. Polymerization of PBTB

2 (214 mg, 0.435 mmol), **5** (85 mg, 0.186 mmol), and 1,4-benzenediboronic acid bis(pinacol)ester (231 mg, 0.7 mmol) were dissolved in THF (20 mL). After degassing, $Pd(PPh_3)_4$ (0.047 g, 0.041 mmol) and 2 M aqueous potassium carbonate solution (12 mL) were added to the reaction mixture. The mixture was then refluxed for 48 h. After cooling, the mixture was poured into excess methanol and the precipitate was washed with acetone, methanol, water, and acetone. After purification, the final, brown solid was obtained to yield 162 mg (53%). ^{1}H NMR (300 MHz, $CDCl_3$) δ(ppm)=8.2-7.3 (m), 7.2-6.8 (m), 5.5-5.0 (m), 4.0 (m), 2.7-1.5 (m), 1.5-1.2 (m), 1.2–0.5 (m). ^{13}C NMR ($CDCl_3$): δ(ppm) =77.00, 31.83, 29.36, 26.13, 22.69, 14.12. FT-IR (cm^{-1}): 2924 (C-H), 1610 (C=C), 1570 (C=C), 1257 (C-N). Anal. Calcd. For $C_{6.43}H_{7.8}N_{0.15}S_{0.08}$: C, 77.2%; H, 7.8%; N, 2.1%; S, 2.4%; Found: C, 78.0%; H, 8.0%; N, 1.9%; S, 2.1%.

2.3. Preparation of CP nanoparticles covered with Pluronic F127 (PBTB-F)

A mixture of PBTB (5 mg) and Pluronic F127 (83 mg) was completely dissolved in THF (1 mL) at 50 °C overnight. Next, deionized water (10 mL) was quickly injected into the mixture under vigorous stirring at 50 °C. After stirring for 5 min, the dispersion was dialyzed against deionized water using a dialysis membrane (MWCO 2 KDa) at 50 °C for 48 h to remove the THF. The resulting nanoparticles (PBTB-F) were isolated by centrifugation at 60,000 rpm for 20 min to remove unencapsulated PBTB and free surfactants. The precipitates were redispersed in deionized water before the characterization and cancer cell study. The concentrations of PBTB used for the subsequent measurements and cell study were calculated from preestablished calibration curve.

2.4. Measurement of ROS generation[38]

ROS generation by PBTB-F was measured using RNO as a ROS indicator and evaluated by a decrease in the UV absorption of RNO at 440 nm. PBTB-F was dissolved in phosphate buffered saline (PBS; 10 mM, pH=7.4) in the presence of RNO (50 μM) and the mixture was then irradiated by a UV lamp (254 nm) at varying power densities for various time periods.

2.5. Cell culture and cytotoxicity test

A typical MTT assay was used. HeLa cells were incubated for 24 h at 37 °C in a μ-slide 8-well microscopy chamber at a density of 1×10^4 cells per well. The cells were incubated with various concentrations of PBTB-F for 12, 24, and 48 h; 10 μL of MTT solution (0.5 mg/mL) was then added and incubated for an additional 4 h. The lysis buffer (20% sodium dodecyl sulfate in 50% aqueous DMF) was added to solubilize the formazan crystal, and the absorbance at 570/630 nm was measured with a microplate reader (Molecular Devices).

2.6. Cell imaging and endogenous test of ROS[39]

HeLa cells were incubated in a μ-slide 8-well microscopy chamber at a density of 1×10^4 cells per well for 24 h at 37 °C. After washing, the cells were incubated with the PBTB-F for 12 h at 37 °C. The cells were then washed with cold PBS buffer and fixed with 4% (w/v) paraformaldehyde solution for 20 min at room temperature. Fluorescence images were obtained using a DeltaVision™ PD system (λ_{ex}=360 nm). For endogenous test of ROS, HeLa cells were prepared as describe above. On the next day, the cells were treated with PBTB-F with various concentrations. After 24 h incubation, the cells were washed with PBS three times and subsequently treated with H2DCFDA (5 μM/well) for 30 min. The cells were washed with PBS and lysed with a cell lysis buffer (Gene Therapy Systems, USA), and then 200 μL of solution from each well was transferred to a 96-well black microplate. The fluorescence intensity resulting from the oxidation of H2DCFDA was quantified (excitation/emission: 488/520 nm) on a SpectroMax M5 microplate reader (Molecular Devices) for the determination of the ROS level.

2.7. Cell viability of PDT effect

A typical MTT assay was used. HeLa cells were incubated in a

 © The Polymer Society of Korea and Springer 2017

μ-slide 8-well microscopy chamber at a density of 1×10^4 cells per well for 24 h at 37 °C. The cells were incubated with different concentrations of PBTB-F for 24 h. After the cells were irradiated using a Spectrolinker XL-1000 UV crosslinker at various power intensities, the cell viabilities of the samples were determined by an MTT test.

3. Results and Discussion

The CP, PBTB, was synthesized by Suzuki-coupling polymerization using a Pd catalyst described in the Experimental section (Scheme 1). The chemical structure of PBTB was confirmed by ^{1}H NMR, ^{13}C NMR, and EA. From the EA data, the molar composition of PBTB was determined to be 0.74:0.26 (m:n). The polymer exhibited good solubility in THF and chloroform because of the presence of long alkyl chains in the polymer structure (maximum solubility: 1.21 mg/mL in chloroform). The molecular weight of PBTB could be obtained with GPC using THF. The number (M_n) and weight-average molecular weight (M_w) of the PBTB were found to be 8430 and 10180 with a polydispersity of 1.21.

UV-vis and fluorescence spectra of PBTB were investigated in chloroform solutions and in the film state (Figure 1). The absorption band of PBTB was observed at 330 nm and a weaker absorption around 500 nm. Different emissions depending on the phases of PBTB (solution or solid) were observed (Figure 1(b)). The fluorescence spectrum of PBTB solution exhibited both blue (420 nm) and red (653 nm) emissions, whereas, in the solid state it showed more intensified red emission at 653 nm. This was caused by the well-known phenomenon of the facilitated intermolecular energy transfer in the solid state.[40-43]

To facilitate the introduction of PBTB into cancer cells, PBTB nanoparticles were prepared by the reprecipitation method and the surface was covered with an amphiphilic block copolymer (Pluronic F127). Because of the hydrophobic interaction between the hydrophobic PBTB and the hydrophobic PO units of Pluronic F127, PBTB-F with a PBTB core and a Pluronic F127 shell was formed (Scheme 2). The spherical shape of the core-shell structure was confirmed with TEM (inset TEM image in Scheme 2). The size of the PBTB-F was measured to be ~192 nm by DLS with a zeta potential of -12.0 mV. To confirm the ability of ROS generation from PBTB-F, a UV lamp (254 nm, 2 W/cm^2) was used as a light source and the ability for $^1O_2$ generation from PBTB-F was quantified using absorption changes in the indicator

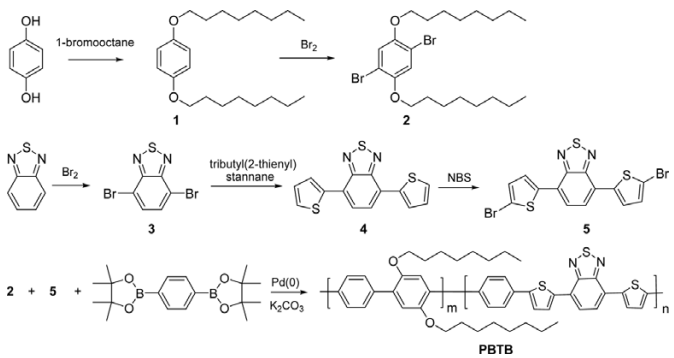

Scheme 1. Synthesis of monomers and polymer.

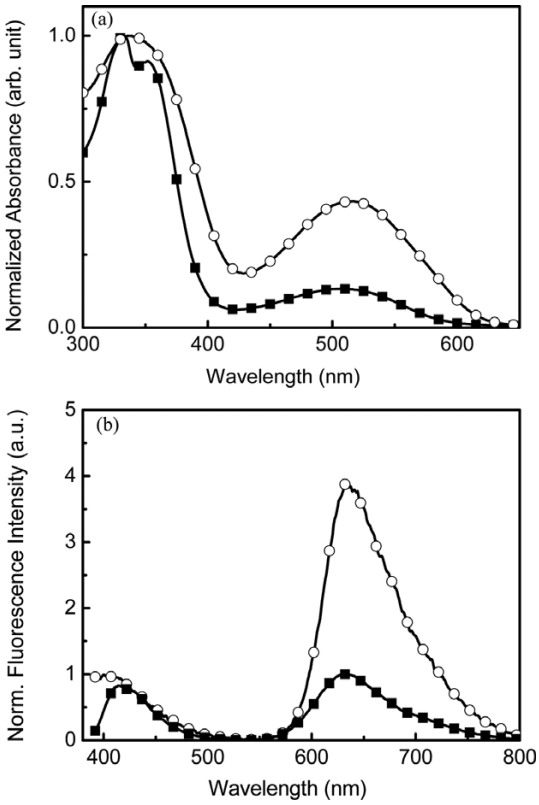

Figure 1. (a) UV-vis and (b) fluorescence spectra of PBTB in chloroform solutions (■) and in the solid film (○). Excitation wavelengths: 330 nm for solution and 370 nm for film.

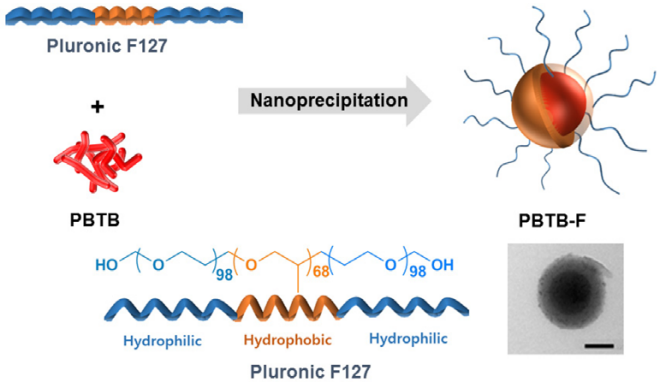

Scheme 2. Fabrication of PBTB-F with core-shell structure prepared with PBTB (core) and Pluronic F127 (shell). TEM image shows a core-shell structure of PBTB-F (scale bar: 100 nm). The chemical structure of Pluronic F127 indicates the amphiphilic nature.

(RNO). As expected, the PBTB-F exhibited a progressive decrease in RNO absorption with prolonged UV irradiation, indicating that PBTB-F could efficiently generate $^1O_2$ under UV irradiation (Figure 2).

To evaluate the biological safety of PBTB-F, its cell viability was investigated using HeLa cells measured by an MTT assay (Figure 3). The results indicated that cell viability was not significantly affected by cell density, concentration of PBTB-F, and incubation time, which indicates the good biocompatibility of PBTB-F. Subsequently, the cell uptake of PBTB-F was carried out by incubation of HeLa cells with PBTB-F for 12 h at various concentrations from 0 to 1800 ng/mL. After incubation, intra-

© The Polymer Society of Korea and Springer 2017

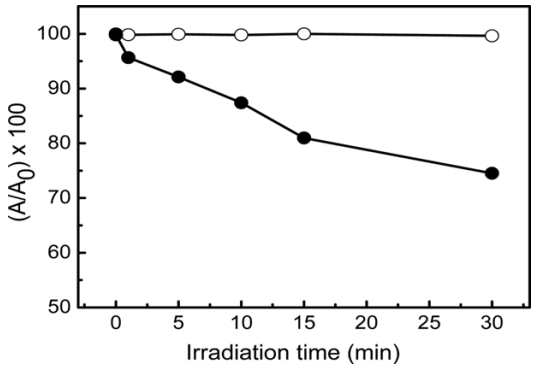

Figure 2. ROS generation after UV irradiation (254 nm) for different time periods in the absence (○) and presence of PBTB-F (●). The amount of $^1O_2$ production was determined by changes in absorbance of RNO (ROS indicator). A_0 and A correspond to the absorbance at 440 nm without and with UV light, respectively. [PBTB-F]=1800 ng/mL.

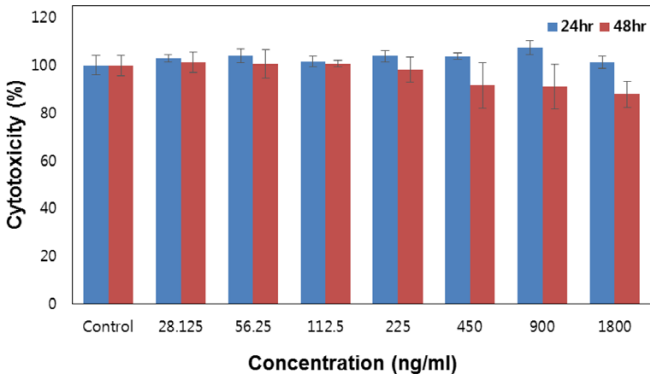

Figure 3. Cytotoxicity test. HeLa cells were incubated at 37 °C for 24 and 48 h with various concentrations of PBTB-F on a 96-well plate at cell density of 1×10^4 cells per well.

cellular fluorescence was clearly observed, versus the control, suggesting that the HeLa cells internalized PBTB-F. The increase in concentration of PBTB-F provided a more defined fluorescence image without cell death (Figure 4). The concentration of PBTB-F (1800 ng/mL) was used for the subsequent ROS test, because most recognizable cell imaging was achieved at this concentration.

The endogenous ROS production in HeLa cells was quantified using the indicator H2DCFDA (Figure 5). The passive uptake of H2DCFDA was followed by diffusion into the cells. The diffused H2DCFDA is oxidized by ROS and the nonfluorescent H2DCFDA became highly fluorescent, which could be quantified using a microplate reader. Therefore, H2DCFDA is commonly used for indicating the quantification of several ROS, including hydroxy radicals, peroxynitrite, and hydrogen peroxide.[39] HeLa cells were incubated with PBTB-F dispersed in the cell culture media for 24 h. The fluorescence intensity of H2DCFDA did not vary with the absence of PBTB-F or the use of low-intensity UV of 0.610 mJ/cm^2 (Figure 5(a)); however, the presence of PBTB-F, an increase in UV-irradiation time, and the use of higher UV intensity provided more efficient ROS production, under which the fluorescence intensity of H2DCFDA increased according to these factors (Figure 5(b)). Interestingly, a decrease in the fluorescence of H2DCFDA was observed after 15 min irradiation under UV light of 100 mJ/cm^2 (Figure 5(c)). This could be interpreted as possible bleaching of the indicator by the intense and prolonged UV irradiation.

Finally, to elucidate the therapeutic efficiency of the PBTB-F under UV light irradiation, an MTT-based in vitro cell viability assay was carried out using HeLa cells (Figure 6). The HeLa cells were incubated with the PBTB-F for 24 h. For unirradi-

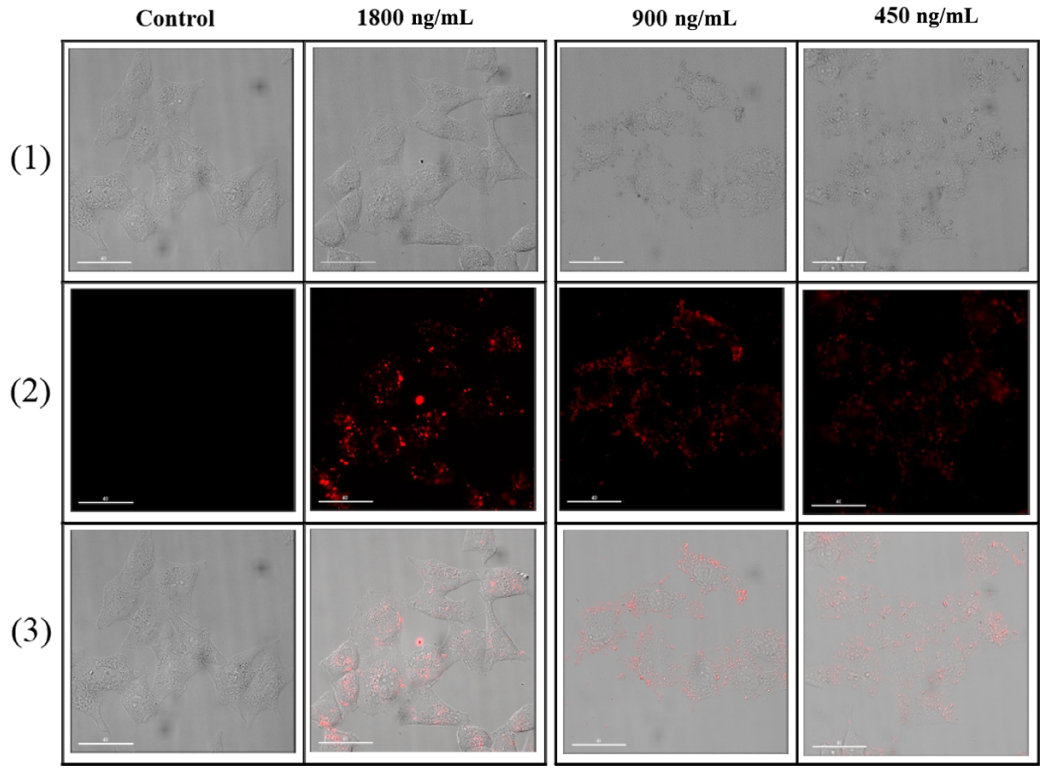

Figure 4. Fluorescence images of HeLa cells incubated with PBTB-F. (1) Bright field; (2) Fluorescent channels; (3) Corresponding overlay images of bright field and fluorescent channels. [PBTB-F]=0, 1800, 900, and 450 ng/mL from left to right. Excitation at 360 nm.

 © The Polymer Society of Korea and Springer 2017

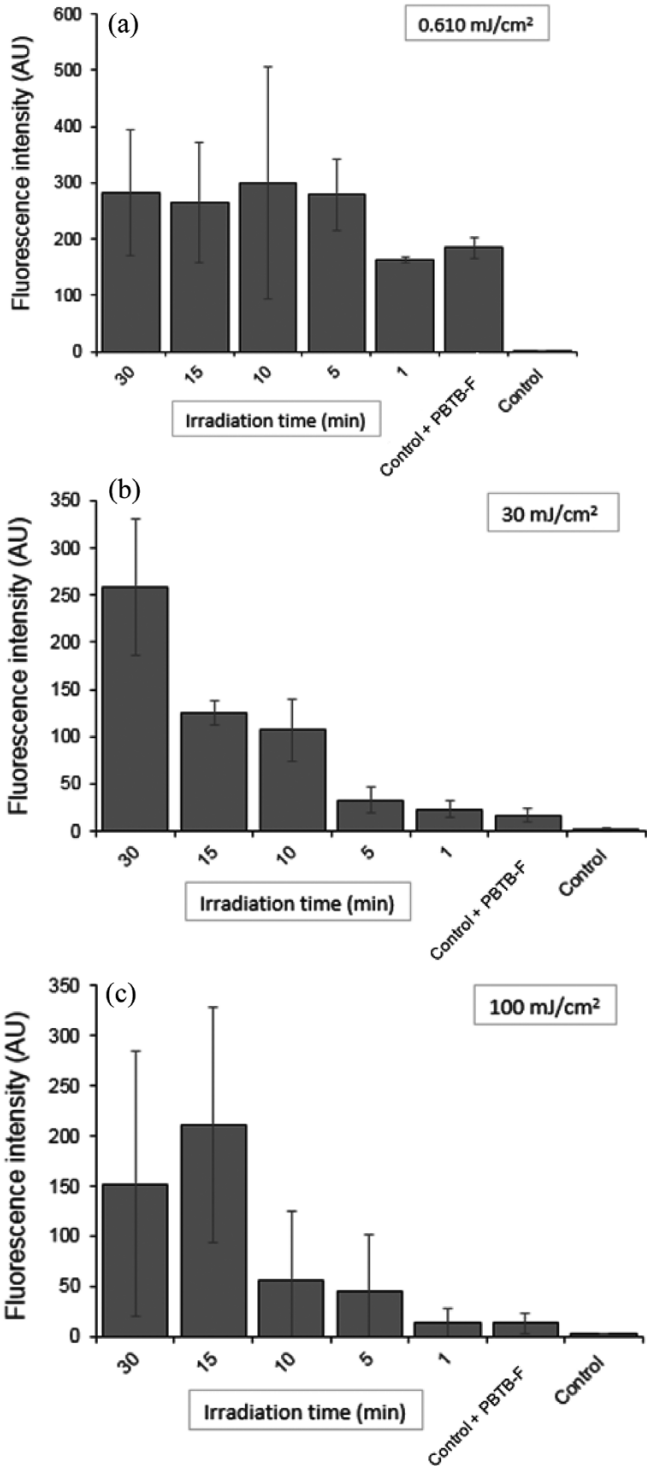

Figure 5. Quantifications of ROS in HeLa cells determined by oxidation of H2DCFDA. [PBTB-F]=1800 ng/mL. The control consisted of cells only. The data were statistically analyzed and significant differences in the ROS levels were determined by monitoring the fluorescence intensity. Intensity of the UV irradiation: (a) 0.610; (b) 30; (c) 100 mJ/cm^2.

ated HeLa cells or for cells with low-intensity (20 mJ/cm^2) UV irradiation, negligible cytotoxicity was observed, irrespective of the presence of PBTB-F, which is indicative of inefficient ROS production. By contrast, when PBTB-F-loaded HeLa cells were irradiated under UV light with higher intensity (30 mJ/cm^2), a remarkable decrease in cell viability (~80%) was observed even

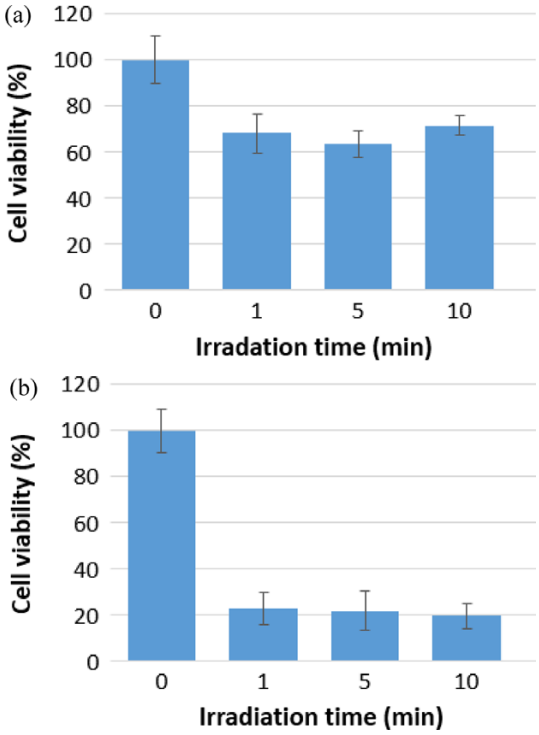

Figure 6. Photodynamic effect of PBTB-F. HeLa cells were incubated with PBTB-F on a 96-well plate at a cell density of 1× 10^4 per well for 24 h at 37 °C. [PBTB-F]=1800 ng/mL. The cell viability was measured *via* MTT assay under UV irradiation with intensity of (a) 20 and (b) 30 mJ/cm^2.

for a short irradiation time (1 min), which indicates good PDT efficiency. Thus, as a multifunctional platform, PBTB-F could attain therapeutic efficiency through PDT, as well as fluorescent imaging of cancer cells.

4. Conclusions

We synthesized CP containing phenylene and benzothiadiazole groups in the main chain. The resulting polymer was made into nanoparticles, that were covered with a polymer surfactant (Pluronic F127), allowing the nanoparticles to be internalized into HeLa cells. The nanoparticles showed low cytotoxicity, good cellular uptake, and efficient ROS generation. As a result, cancer cell imaging was accomplished when the nanoparticles were introduced into the HeLa cells. The nanoparticles exhibited a photodynamic effect, facilitating apoptosis of cancer cells. Thus, these nanoparticles have the potential for wide applications in the diagnostic and medical fields for cell imaging and therapy, in which cancer cells are subjected to illumination under an appropriate light source.

References

(1) J. Folkman, *Nat. Med.*, **1**, 27 (1995).
(2) P. Anand, A. B. Kunnumakara, C. Sundaram, K. B. Harikumar, S. T. Tharakan, O. S. Lai, B. Sung, and B. B. Aggarwal, *Pharm. Res.*, **25**, 2097 (2008).
(3) S. A. Newell, A. Girgis, R. W. Sanson-Fisher, N. J. Savolainen, and B. Hons, *Am. J. Prev. Med.*, **17**, 211 (1999).
(4) J. Lin, S. Wang, P. Huang, Z. Wang, S. Chen, G. Niu, W. Li, J. He, D. Cui, G.

© The Polymer Society of Korea and Springer 2017

Lu, X. Chen, and Z. Nie, *ACS Nano*, **7**, 5320 (2013).
(5) E. Paszko, C. Ehrhardt, M. O. Senge, D. P. Kelleher, and J. V. Reynolds, *Photodiagnosis Photodyn. Ther.*, **8**, 14 (2011).
(6) D. E. J. G. J. Dolmans, D. Fukumura, and R. K. Jain, *Nat. Rev. Cancer*, **3**, 380 (2003).
(7) E. B. Ku, K. T. Oh, Y. S. Youn, and E. S. Lee, *Macromol. Res.*, **24**, 634 (2016).
(8) A. P. Castano, P. Mroz, and M. R. Hamblin, *Nat. Rev. Cancer*, **6**, 535 (2006).
(9) C. M. Peterson, J. M. Lu, Y. Sun, C. A. Peterson, J. Shiah, R. C. Straight, and J. Kopeček, *Cancer. Res.*, **56**, 3980 (1996).
(10) A. Khdair, D. Chen, Y. Patil, L. Ma, Q. P. Dou, M. P. V. Shekhar, and J. Panyam, *J. Control. Release*, **141**, 137 (2010).
(11) K. J. Son, H. Yoon, J. Kim, W. Jang, Y. Lee, and W. Koh, *Angew. Chem. Int. Ed.*, **50**, 11968 (2011).
(12) S. H. Kang, M. Nafiujjaman, M. Nurunnabi, L. Li, H. A. Khan, K. J. Cho, K. M. Huh, and Y. Lee, *Macromol. Res.*, **23**, 474 (2015).
(13) J. Pecher and S. Mecking, *Chem. Rev.*, **110**, 6260 (2010).
(14) C. Zhu, L. Liu, Q. Yang, F. Lv, and S. Wang, *Chem. Rev.*, **112**, 4687 (2012).
(15) D. Kim and T. S. Lee, *ACS Appl. Mater. Interfaces*, **8**, 34770 (2016).
(16) Y. J. Jin, J. H. Oh, and G. Kwak, *Polym. Korea*, **40**, 736 (2016).
(17) L. Feng, C. Zhu, H. Yuan, L. Liu, F. Lv, and S. Wang, *Chem. Soc. Rev.*, **42**, 6620 (2013).
(18) R. Duncan, *Nat. Rev. Cancer*, **6**, 688 (2006).
(19) L. Feng, J. Zhu, and Z. Wang, *ACS Appl. Mater. Interfaces*, **8**, 19364 (2016).
(20) S. Chemburu, T. S. Corbitt, L. K. Ista, E. Ji, J. Fulghum, G. P. Lopez, K. Ogawa, K. S. Schanze, and D. G. Whitten, *Langmuir*, **24**, 11053 (2008).
(21) C. Xing, L. Liu, H. Tang, X. Feng, Q. Yang, S. Wang, and G. C. Bazan, *Adv. Funct. Mater.*, **21**, 4058 (2011).
(22) E. Ji, T. S. Corbitt, A. Parthasarathy, K. S. Schanze, and D. G. Whitten, *ACS Appl. Mater. Interfaces*, **3**, 2820 (2011).
(23) C. Zhu, Q. Yang, F. Lv, L. Liu, and S. Wang, *Adv. Mater.*, **25**, 1203 (2013).
(24) Y. Yuan, J. Liu, and B. Liu, *Angew. Chem. Int. Ed.*, **126**, 7291 (2014).
(25) S. Li, K. Chang, K. Sun, Y. Tang, N. Cui, Y. Wang, W. Qin, H. Xu, and C. Wu, *ACS Appl. Mater. Interfaces*, **8**, 3624 (2016).
(26) D. Gao, R. R. Agayan, H. Xu, M. A. Philbert, and R. Kopelman, *Nano Lett.*, **6**, 2383 (2006).
(27) K. Li and B. Liu, *J. Mater. Chem.*, **22**, 1257 (2012).
(28) J. Yu, C. Wu, S. P. Sahu, L. P. Fernando, C. Szymanski, and J. McNeill, *J. Am. Chem. Soc.*, **131**, 18410 (2009).
(29) X. Zhou, H. Liang, P. Jiang, K. Y. Zhang, S. Liu, T. Yang, Q. Zhao, L. Yang, W. Lv, Q. Yu, and W. Huang, *Adv. Sci.*, **3**, 1500155 (2016).
(30) H. Shi, X. Ma, Q. Zhao, B. Liu, Q. Qu, Z. An, Y. Zhao, and W. Huang, *Adv. Funct. Mater.*, **24**, 4823 (2014).
(31) A. Pitto-Barry and N. P. E. Barry, *Polym. Chem.*, **5**, 3291 (2014).
(32) A. V. Kabanov, E. V. Batrakova, and V. Y. Alakhov, *J. Control. Release*, **82**, 189 (2002).
(33) A. V. Kabanov, E. V. Batrakova, and D. W. Miller, *Adv. Drug Deliv. Rev.*, **55**, 151 (2003).
(34) A. V. Kabanov, P. Lemieux, S. Vinogradov, and V. Alakhov, *Adv. Drug Deliv. Rev.*, **54**, 223 (2002).
(35) L. Oktavia, S. J. Kim, J. H. Kim, H. Park, C. W. Lee, and M. Kwak, *Polym. Korea*, **40**, 130 (2016).
(36) R. Yang, R. Tian, J. Yan, Y. Zhang, J. Yang, Q. Hou, W. Yang, C. Zhang, and Y. Cao, *Macromolecules*, **38**, 244 (2005).
(37) Q. Hou, Y. Xu, W. Yang, M. Yuan, J. Peng, and Y. Cao, *J. Mater. Chem.*, **12**, 2887 (2002).
(38) Z. Hu, F. Zhao, Y. Wang, Y. Huang, L. Chen, N. Li, J. Li, Z. Lia, and G. Yi, *Chem. Commun.*, **50**, 10815 (2014).
(39) A. Chompoosor, K. Saha, P. S. Ghosh, D. J. Macarthy, O. R. Miranda, Z. Zhu, K. F. Arcaro, and V. M. Rotello, *Small*, **6**, 2246 (2010).
(40) G. Jang, S. Seo, and T. S. Lee, *Sens. Actuat. B: Chem.*, **221**, 1229 (2015).
(41) G. Klärner, J. Lee, M. H. Davey, and R. D. Miller, *Adv. Mater.*, **11**, 115 (1999).
(42) E. Hennebicq, G. Pourtois, G. D. Scholes, L. M. Herz, D. M. Russell, C. Silva, S. Setayesh, A. C. Grimsdale, K. Mullen, J. Bredas, and D. Beljonne, *J. Am. Chem. Soc.*, **127**, 4744 (2005).
(43) M. Ariu, M. Sims, M. D. Rahn, J. Hill, A. M. Fox, and D. G. Lidzey, *Phys. Rev. B*, **67**, 195333 (2003).

 © The Polymer Society of Korea and Springer 2017